

An efficient Jacobian scaling method for time-domain optical mammography

Yiwen Ma (马艺闻)^{1,2*}, Feng Gao (高峰)², Pingqiao Ruan (阮平巧)²,
Fang Yang (杨芳)², and Huijuan Zhao (赵会娟)²

¹State Key Laboratory of Precision Measuring Technology and Instruments, Tianjin University,
Tianjin 300072, China

²College of Precision Instrument and Optoelectronics Engineering, Tianjin University,
Tianjin 300072, China

*E-mail: yiwenma@tju.edu.cn

Received April 27, 2009

Time-domain diffuse optical tomography can efficiently reconstruct optical parameters which can be further applied in diagnosing early breast cancer. Nevertheless, the performances of reconstructed imaging are badly influenced by different Jacobian magnitudes of absorption coefficient and reduced scattering coefficient. With the introduction of a relative data type based on generalized pulse spectrum technique, an efficient Jacobian scaling method is proposed. The interrelated simulated validation is also revealed for the enhancing performances.

OCIS codes: 100.3010, 170.3830, 300.6500.

doi: 10.3788/COL20100802.0206.

Early detection is quite significant for improving the curative ratio of breast cancer and reducing its mortality^[1]. As a new noninvasive optical measurement technique, optical mammography of diffuse optical tomography (DOT) has attracted much attention for providing a richer functional image^[2–6]. Based on the sensitive connection between light and the physiological index, time-domain DOT can efficiently reconstruct the optical parameters of breast tissue by measuring the boundary flux with a time-resolved system. Although the ill-posed problems of the inverse problem have a very bad effect on the quality of the reconstructed image, regularization of ill-posed problems can provide a better reconstructed image^[7]. However, this method requires complicated computation.

In view of the marked magnitude differences in absorption coefficient and reduced scattering coefficient^[8], we propose an efficient scaling method of the Jacobian matrix that can improve the performance of the reconstructed image in this letter. To avoid the absolute system scaling, a relative data type^[8,9] is used here. The scaling method of the Jacobian matrix according to the data type is proposed with an interrelated simulated validation.

In time-domain DOT, the photon-migration model in the tissue is prevalently described by the diffusion approximation (DA) to the Boltzman transport equation. To simplify the calculation of the diffuse equation, the generalized pulse spectrum technique (GPST) is introduced^[6,8,9]. Based on converting the time-dependent signals by the Laplace transform to a real frequency domain^[5], this technique can make the solving of the time-domain diffuse equation from a 4-dimensional (4D) space-time problem into a 3-dimensional (3D) one. The detailed solving process of the forward problem using Galerkin finite element method (FEM) can be found

in Ref. [9], when the GPST is adopted in time-domain DOT. The nonlinear inverse problem posed by DOT can be linearized by a Newton-Raphson scheme^[8,10], which forms an outer-loop of the iterative procedure expressed as

$$\begin{aligned}\delta\Gamma &= [\Gamma - F(x_k)] = J(x_k)\delta x_k, \\ x_{k+1} &= x_k + \delta x_k,\end{aligned}\quad (1)$$

where Γ is a column vector of length $S \times D$ ^[9] (S represents the number of sources and D represents the number of detectors), numerating the Laplace-transformed re-emissions for all source-detector pairs, F is the forward operator associated with the photon diffusion equation, x_k and δx_k are the vectors denoting the optical properties (both the absorption and reduced scattering coefficients) at the nodes of the FEM mesh and their perturbations, at the k th updating state, and $J(x)$ is the Jacobian matrix of F , which can be written as $J(x) = [J_a, J_s]$ where J_a and J_s correspond to the changes in the absorption and reduced scattering coefficients.

According to the modified GPST^[8,9], the Jacobian matrices, J_a and J_s , have the following relations in each FEM element:

$$J_{s,e}(\xi_d, \zeta_s, p) = J_{a,e}(\xi_d, \zeta_s, p) \times \frac{\overline{\mu_{a,e}} + \frac{p}{c}}{\overline{\mu'_{s,e}}}, \quad (2)$$

where $\overline{\mu_{a,e}}$ and $\overline{\mu'_{s,e}}$ are the average values of the absorption and reduced scattering coefficients in the e th FEM element, respectively, $J_{a,e}(\xi_d, \zeta_s, p)$ and $J_{s,e}(\xi_d, \zeta_s, p)$ are Jacobian matrices of the absorption and reduced scattering coefficients in the e th FEM element, respectively, p is the Laplace-transformed factor, and c is the velocity of light in tissue.

To avoid the absolute system scaling when the intensity-related signals are employed, a relative data

type, $R(\xi_d, \zeta_s) = \Gamma(\xi_d, \zeta_s, p_2) / \Gamma(\xi_d, \zeta_s, p_1)$ ^[8–9], is used in this letter, where $\Gamma(\xi_d, \zeta_s, p_1)$ and $\Gamma(\xi_d, \zeta_s, p_2)$ are the photon flux where ξ_d and ζ_s are the detector and source positions. Suppose that $J_{a,e}^R(\xi_d, \zeta_s)$ and $J_{s,e}^R(\xi_d, \zeta_s)$ are the Jacobian matrices of absorption and reduced scattering coefficients regarding $R(\xi_d, \zeta_s)$ in the e th FEM element, and then $J_{a,e}^R(\xi_d, \zeta_s)$ and $J_{s,e}^R(\xi_d, \zeta_s)$ are accordingly reformularized as

$$J_{a,e}^R(\xi_d, \zeta_s) = \frac{1}{\Gamma(\xi_d, \zeta_s, p_1)} \times [J_{a,e}(\xi_d, \zeta_s, p_2) - R \times J_{a,e}(\xi_d, \zeta_s, p_1)], \quad (3)$$

$$J_{s,e}^R(\xi_d, \zeta_s) = \frac{1}{\Gamma(\xi_d, \zeta_s, p_1)} [J_{s,e}(\xi_d, \zeta_s, p_2) \times \frac{\overline{\mu_{a,e}} + \frac{p_2}{c}}{\mu'_{s,e}} - R \frac{\overline{\mu_{a,e}} + \frac{p_1}{c}}{\mu'_{s,e}} \times J_{a,e}(\xi_d, \zeta_s, p_1)]. \quad (4)$$

When μ_a^B is the absorption coefficient of the background, and two Laplace-transformed factors are chosen as $p_1 = -0.5\mu_a^B c$ and $p_2 = 0.5\mu_a^B c$ (To simplify the reconstruction process, the working frequencies are set to be in the real domain), Eq. (4) can be written as

$$J_{s,e}^R(\xi_d, \zeta_s) = \frac{1}{\Gamma(\xi_d, \zeta_s, p_1)} [J_{a,e}(\xi_d, \zeta_s, p_2) \times \frac{\overline{\mu_{a,e}} + 0.5\mu_a^B}{\mu'_{s,e}} - R \frac{\overline{\mu_{a,e}} - 0.5\mu_a^B}{\mu'_{s,e}} \times J_{a,e}(\xi_d, \zeta_s, p_1)]. \quad (5)$$

Assuming that μ_s^B is the reduced scattering coefficient of the background, $\frac{\mu'_{s,e}}{\mu_s^B} \approx \mu_s^B$, $\overline{\mu_{a,e}} \approx \mu_a^B$, and $\mu_s^B = AM \cdot \mu_a^B$ (AM is a scaling factor), we can obtain the relation of $\frac{\mu'_{s,e}}{\mu_s^B} \approx AM \cdot \overline{\mu_{a,e}}$ in any FEM element. When both $J_{a,e}(\xi_d, \zeta_s, p_1)$ and $J_{a,e}(\xi_d, \zeta_s, p_2)$ are greater than zero, the value range of $J_{s,e}^R(\xi_d, \zeta_s)$ can be derived as $[\frac{1}{2AM} J_{a,e}^R(\xi_d, \zeta_s), \frac{3}{2AM} J_{a,e}^R(\xi_d, \zeta_s)]$. Since the value of AM of breast tissue is far superior to 1^[11], we know that the Jacobian matrix of $J_{a,e}^R(\xi_d, \zeta_s)$ is several orders of magnitudes larger than that of $J_{s,e}^R(\xi_d, \zeta_s)$. This magnitude difference results in the μ_a -reconstruction more pronounced and the simultaneous reconstruction of both the μ_a μ_s' being unbalanced. To enhance the efficiency of the modified GPST algorithm in μ_s' -reconstruction using the algebraic reconstruction technique (ART), a scaling strategy that divided by the maximum element along a row of the Jacobian matrix^[8] can be used to equalize the Jacobian matrix. Owing to the uncertainty of the Jacobian matrix, we still cannot get a perfect reconstruction of μ_s' according to the above scaling method.

Considering that the reduced scattering coefficient is closely related with tissue of different forms, and that the abnormality tissue has great variation in reduced scattering coefficient, the efficiently reconstructed image of μ_s' can provide more diagnosis information^[12]. According to the suppositions and relations of Jacobian matrix in Eqs. (3) and (5), we can conclude that the ratio of $J_{a,e}^R(\xi_d, \zeta_s)$ and $J_{s,e}^R(\xi_d, \zeta_s)$ is in connection with μ_a^B and μ_s^B . Based on this, we present an improved Jacobian

scaling method where the Jacobian matrix is multiplied by the background optical parameters.

Using our scaling method, the scaling Jacobian matrices of μ_a and μ_s' in the e th element can be written as

$$\begin{cases} J'_{a,e}{}^R(\xi_d, \zeta_s) = \mu_a^B J_{a,e}^R(\xi_d, \zeta_s) \\ J'_{s,e}{}^R(\xi_d, \zeta_s) = \mu_s^B J_{s,e}^R(\xi_d, \zeta_s) \end{cases}, \quad (6)$$

where $J'_{a,e}{}^R(\xi_d, \zeta_s)$ and $J'_{s,e}{}^R(\xi_d, \zeta_s)$ are the scaling Jacobian matrices of μ_a and μ_s' regarding $R(\xi_d, \zeta_s)$ in the e th FEM element, and then the new Jacobian matrices can be obtained accordingly as

$$\begin{cases} J'_{a,e}{}^R(\xi_d, \zeta_s) = \frac{\mu_a^B [J_{a,e}(\xi_d, \zeta_s, p_2) - R \times J_{a,e}(\xi_d, \zeta_s, p_1)]}{\Gamma(\xi_d, \zeta_s, p_1)} \\ J'_{s,e}{}^R(\xi_d, \zeta_s) = \left\{ \mu_s^B [J_{s,e}(\xi_d, \zeta_s, p_2) \times \frac{\overline{\mu_{a,e}} + 0.5\mu_a^B}{\mu'_{s,e}} - R \frac{\overline{\mu_{a,e}} - 0.5\mu_a^B}{\mu'_{s,e}} \times J_{a,e}(\xi_d, \zeta_s, p_1)] \right\} / \Gamma(\xi_d, \zeta_s, p_1) \end{cases}. \quad (7)$$

It can be seen that $J'_{a,e}{}^R$ and $J'_{s,e}{}^R$ are now in the same magnitude order. It is noted that the reconstructed optical properties need to be de-equalized after the reconstruction.

The validation of this Jacobian scaling method is conducted in a 3D test object, as shown in Fig. 1. The 3D test object is a cylinder with radius of $R = 30$ mm and height of $H = 30$ mm. The background optical properties of this cylinder are $\mu_a = 0.004$ mm⁻¹, $\mu_s' = 1$ mm⁻¹ (which are near the optical parameters of breast tissue). Two little cylinders, with a center-to-center separation (CCS) of 20 mm and optical properties of $\mu_a = 0.01$ mm⁻¹ and $\mu_s' = 1.8$ mm⁻¹ (which are near the optical parameters of breast tumor), radius of $r_i = 5$ mm ($i = 1, 2$), and height of $h_i = 10$ mm ($i = 1, 2$), are embedded along the y -axis to simulate two tumor targets. Sixty-four coaxial source-detector optodes ($S = D = 64$) are arranged in four layers to achieve the best experimental effect, i.e., each layer has sixteen optodes. To apply the FEM, the cylindrical phantom is divided into 151200 tetrahedron elements that join at 27742 nodes.

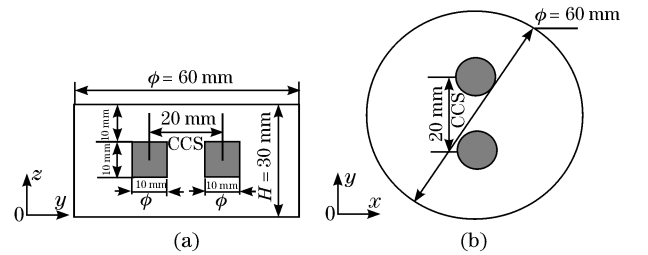


Fig. 1. Geometric sketch of the phantom. (a) Sagittal-section of the phantom; (b) cross-section of the phantom.

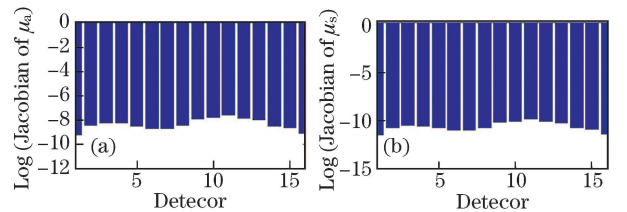


Fig. 2. Logarithm of Jacobian values of (a) absorption coefficient and (b) reduced scattering coefficient with respect to the relative data type at 16 detectors by the bars.

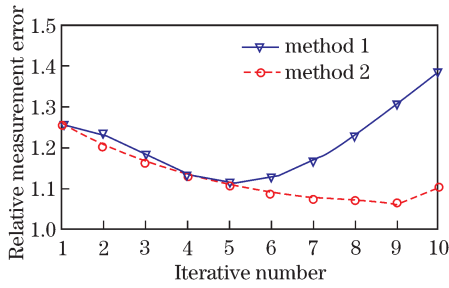


Fig. 3. Relative measurement errors as a function of iterative number in two Jacobian scaling methods with SNR = 40 dB.

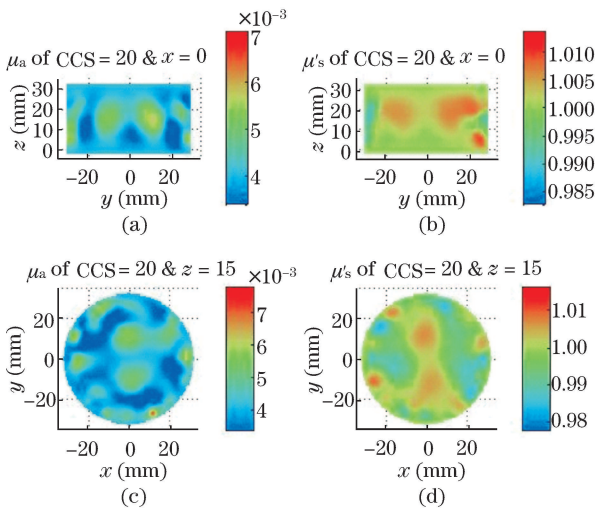


Fig. 4. Sagittal-section and cross-section of reconstructed images with the Jacobian matrix divided by its maximum at SNR = 40 dB. Sagittal-section of reconstructed image of (a) μ_a and (b) μ'_s . Cross-section of reconstructed image of (c) μ_a and (d) μ'_s .

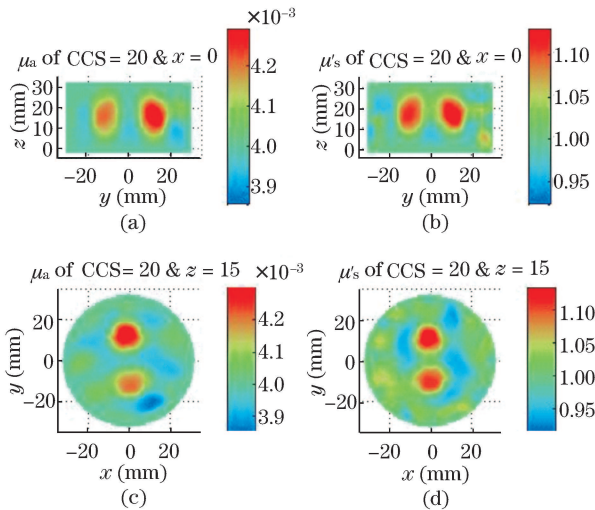


Fig. 5. Sagittal-section and cross-section of reconstructed images with the Jacobian matrix multiplied by the background optical parameter at SNR = 40 dB. Sagittal-section of reconstructed image of (a) μ_a and (b) μ'_s . Cross-section of reconstructed image of (c) μ_a and (d) μ'_s .

In the simulation experiment, a pair of real transform-factors are set as $p_{1,2} = \pm 0.5\mu_a c$, the relaxation parameter of ART is $\lambda = 0.1$, and the stopping iteration number

is $N = 10$. Considering that the tumor has higher optical parameters than the normal tissue, the lower limit factor $\alpha = 0.85$ is introduced in the simulation. In order to reveal the virtue of our Jacobian scaling method, the image is reconstructed in two Jacobian scaling methods with 40-dB signal-to-noise ratio (SNR).

When optodes 1 is lighting, the logarithms of magnitude difference of Jacobian matrices regarding μ_a and μ'_s at 16 detectors of the same layer are shown in Fig. 2 by the bars. Figure 2(a) represents the logarithm of Jacobian value of absorption coefficient with respect to the relative data type at 16 detectors by the bars, and Fig. 2(b) represents the corresponding one of reduced scattering coefficient. It's obviously that the Jacobian matrix of μ_a is several orders of magnitudes larger than that of μ'_s .

For the purpose of comparing the convergence performances of the two Jacobian scaling methods, Fig. 3 shows the relative measurement errors as a function of iterative number in two Jacobian scaling methods with SNR = 40 dB. The solid line represents the scaling method 1 where the Jacobian matrix is divided by its maximum according to Ref. [8], meanwhile, the dashed line represents the scaling method 2 where the Jacobian matrix is multiplied by the background optical parameter. It is implied in Fig. 3 that the Jacobian scaling method 2 proposed in this letter has a better downward tendency and a lower relative measurement error.

Figure 4 illustrates the target images in the sagittal-section and in the cross-section when the iterative number is 5 by the scaling method 1 with SNR = 40 dB. Meanwhile, Fig. 5 shows the reconstructed target images in the same section with the scaling method 2 where the Jacobian matrix is multiplied by the background optical coefficient when the iterative number is 9 and SNR is 40 dB.

For the evaluation on the performances of the reconstructed image with the above two scaling methods with SNR = 40 dB, the profiles of targets along y -axis orientation when $z = 20$ mm and $x = 0$ mm are shown in Fig. 6. The solid line represents the profiles of the original targets. Scaling 1 and 2 of the legend represent the results of the scaling method 1 and 2, respectively.

It is clearly shown in Fig. 6 that compared with the scaling method 1, the scaling method 2 we present here exhibits several advantages including 1) improved quantitative accuracy of the scattering image; 2) better spatial resolution of the reconstructed image both in μ_a and μ'_s ; 3) efficient restraints on the unbalance of μ_a and μ'_s ; 4) better outlines of μ_a and μ'_s ; 5) better noise performance.

In conclusion, a new scaling method of Jacobian matrix

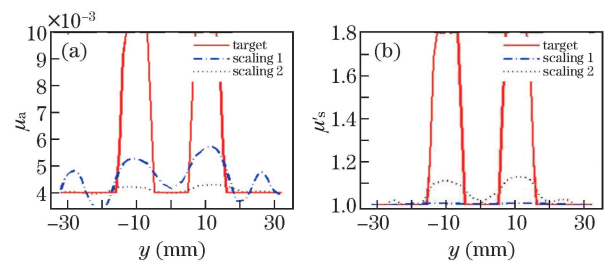


Fig. 6. Profiles of targets along y -axis orientation when $z = 20$ mm and $x = 0$ mm. (a) μ_a ; (b) μ'_s .

for efficiently reconstruction of absorption and reduced scattering coefficients of TR-DOT, based on modified generalized pulse spectrum technique and relative data type, is presented. Unlike the scaling method 1 in Ref. [8], the scaling method 2 can reveal better performance of reconstructed image by efficiently restraining the unbalance of absorption and reduced scattering coefficients. The unbalance of absorption and reduced scattering coefficients is evidently restrained by the background optical parameter which is chosen as the Jacobian scaling factors. Accordingly, the scaling method that Jacobian matrix is multiplied by the background optical parameter can provide a better reconstructed image by improving the ill-posed problems of the inverse problem. The validity of scaling method 2, where the Jacobian matrix is multiplied by 40-dB SNR, is proved. Compared with the scaling method 1, the reconstructed results of the scaling method 2 have demonstrated an evident improvement both in the quality of scattering image and in the spatial resolution of absorption and reduced scattering coefficients.

This work was supported by the National Natural Science Foundation of China (Nos. 30870657 and 30970775), the National Basic Research Program of China (No. 2006CB705700), the Chinese National Programs for High Technology Research and Development (No. 2009AA02Z413), and Tianjin Municipal Government of China (No. 09JCZDJC18200).

References

1. D. R. Leff, O. J. Warren, L. C. Enfield, A. Gibson, T. Athanasiou, D. K. Patten, J. Hebden, G. Z. Yang, and A. Darzi, *Breast Cancer Res. Treat.* **108**, 9 (2008).
2. L. C. Enfield, A. P. Gibson, N. L. Everdell, D. T. Delpy, M. Schweiger, S. R. Arridge, C. Richardson, M. Keshtgar, M. Douek, and J. C. Hebden, *Appl. Opt.* **46**, 3628 (2007).
3. Q. Zhang, T. J. Brukilacchio, A. Li, J. J. Stott, T. Chaves, E. Hillman, T. Wu, M. Chorlton, E. Rafferty, R. H. Moore, D. B. Kopans, and D. A. Boas, *J. Biomed. Opt.* **10**, 024033 (2005).
4. A. P. Gibson, J. C. Hebden, and S. R. Arridge, *Phys. Med. Biol.* **50**, R1 (2005).
5. F. Gao, Y. Xue, H. Zhao, T. Kusaka, M. Ueno, and Y. Yamada, *Chin. Opt. Lett.* **5**, 472 (2007).
6. F. Yang, Y. Ma, F. Gao, and H. Zhao, *Acta Opt. Sin. (in Chinese)* **28**, 1571 (2008).
7. A. R. Zirak and M. Khademi, *Opt. Commun.* **279**, 273 (2007).
8. H. Zhao, F. Gao, Y. Tanikawa, and Y. Yamada, *J. Biomed. Opt.* **12**, 062107 (2007).
9. F. Gao, H. Zhao, Y. Tanikawa, and Y. Yamada, *IEEE Trans. Inf. & Syst.* **E85**, 133 (2002).
10. S. R. Arridge, *Inverse Probl.* **15**, R41 (1999).
11. T. Durduran, R. Choe, J. P. Culver, L. Zubkov, M. J. Holboke, J. Giammarco, B. Chance, and A. G. Yodanis, *Phys. Med. Biol.* **47**, 2847 (2002).
12. K. Xu, F. Gao, and H. Zhao, *Biomedical Photonics (in Chinese)* (Science Press, Beijing, 2007).